

# Low expression of hexokinase-2 is associated with false-negative FDG–positron emission tomography in multiple myeloma

Leo Rasche<sup>1\*</sup>, Edgardo Angtuaco<sup>2\*</sup>, James E. McDonald<sup>2</sup>, Amy Buros<sup>1</sup>, Caleb Stein<sup>1</sup>, Charlotte Pawlyn<sup>3</sup>, Sharmilan Thanendrarajan<sup>1</sup>, Carolina Schinke<sup>1</sup>, Rohan Samant<sup>2</sup>, Shmuel Yaccoby<sup>1</sup>, Brian A. Walker<sup>1</sup>, Joshua Epstein<sup>1</sup>, Maurizio Zangari<sup>1</sup>, Frits van Rhee<sup>1</sup>, Tobias Meissner<sup>4</sup>, Hartmut Goldschmidt<sup>5</sup>, Kari Hemminki<sup>6,7</sup>, Richard Houlston<sup>3</sup>, Bart Barlogie<sup>1</sup>, Faith E. Davies<sup>1</sup>, Gareth J. Morgan<sup>1†</sup>, Niels Weinhold<sup>1†</sup>

1. *Myeloma Institute and*

2. *Radiology Department, University of Arkansas for Medical Sciences, Little Rock, AR;*

3. *The Institute of Cancer Research, London, United Kingdom;*

4. *Department of Molecular and Experimental Medicine, Avera Cancer Institute, Sioux Falls, SD;*

5. *Department of Internal Medicine V, University of Heidelberg, Heidelberg, Germany;*

6. *Division of Molecular Genetic Epidemiology, German Cancer Research Center (DKFZ), Heidelberg, Germany; and*

7. *Center for Primary Health Care Research, Lund University, Malmo, Sweden*

\*. L.R. and E.A. contributed equally to this study.

†. G.J.M. and N.W. jointly directed this study.

© 2017 by The American Society of Hematology

DOI: 10.1182/blood-2017-03-774422

Published in print: 6 July 2017

See "[Toward a GEP-based PET in myeloma.](#)" in volume 130 on page 2.

## Abstract

**Publisher's Note:** There is an Inside *Blood* Commentary on this article in this issue.

## Key Points

- PET false-negativity was seen in 11% of MM patients.
- PET false-negativity was associated with low hexokinase-2 expression.

## Abstract

<sup>18</sup>F-Fluorodeoxyglucose (FDG)–positron emission tomography (PET) and diffusion-weighted magnetic resonance imaging with background signal suppression (DWIBS) are 2 powerful functional imaging modalities in the evaluation of malignant plasma cell (PC) disease multiple myeloma (MM). Preliminary observations have suggested that MM patients with extensive disease according to DWIBS may be reported as being disease-free on FDG-PET (“PET false-negative”). The aim of this study was to describe the proportion of PET false-negativity in a representative set of 227 newly diagnosed MM patients with simultaneous assessment of FDG-PET and DWIBS, and to identify tumor-intrinsic features associated with this pattern. We found the incidence of PET false-negativity to be 11%. Neither tumor load–associated parameters, such as degree of bone marrow PC infiltration, nor the PC proliferation rate were associated with this subset. However, the gene coding for hexokinase-2, which catalyzes the first step of glycolysis, was significantly lower expressed in PET false-negative cases (5.3-fold change,  $P < .001$ ) which provides a mechanistic explanation for this feature. In conclusion, we demonstrate a relevant number of patients with FDG-PET false-negative MM and a strong association between hexokinase-2 expression and this negativity: a finding which may also be relevant for clinical imaging of other hematological cancers.

## Introduction

<sup>18</sup>F-Fluorodeoxyglucose (FDG)–positron emission tomography (PET) and the recently introduced diffusion-weighted magnetic resonance imaging with background signal suppression (DWIBS) are powerful functional imaging modalities in the evaluation of multiple myeloma (MM).<sup>1</sup> These techniques rely on different molecular features with FDG-PET being based not only on the quantification of increased glucose uptake by tumor cells but also by others such as inflammatory cells, whereas in DWIBS the bone marrow (BM) cellularity is measured by quantifying the molecular diffusion of body water and the microcirculation of blood in the capillary network.<sup>2</sup>

Recently published results of a pilot study that examined 17 patients with paired imaging data suggest that patients with extensive disease on DWIBS may be reported as being disease-free on FDG-PET (“PET false-negative”).<sup>3</sup> Because FDG-PET is increasingly being used as a diagnostic tool in MM,<sup>1,4</sup> a further characterization of this phenomenon is essential.

The aim of this study was to describe the proportion of PET false-negative patients and to identify tumor-intrinsic features associated with PET false-negativity. Here, we report on 227 MM patients for whom FDG-PET and DWIBS were simultaneously performed; malignant plasma cells (PCs) were characterized using fluorescence in situ hybridization (FISH) and gene expression profiling (GEP).

## Study design

We investigated 227 transplant-eligible newly diagnosed MM patients using simultaneous FDG-PET and DWIBS, as well as FISH and GEP. This study was approved by the institutional review board (#205415). All patients signed written consent in accordance with the Declaration of Helsinki.

FDG-PET was performed on a Biograph, Reveal, or Discovery scanner. DWIBS was performed on a 1.5 Tesla Philips Achieva scanner. A focal lesion (FL) was defined as a circumscribed focus with increased FDG uptake compared with its surroundings. Diffuse disease (moderate or severe intensity) was defined as previously published.<sup>8</sup> For DWIBS, a FL was defined as well-delineated focal intensity above the surrounding background BM  $\geq$  1 cm in size; diffuse infiltration was defined as intensity above background (details in supplemental Methods, available on the *Blood* Web site).

The scans were reported by 2 independent radiologists and 1 nuclear medicine physician who were blinded to the clinical information, and other imaging results. Presence of disease was defined as diffuse and/or focal activity. We assigned patients to the following groups: disease detectable by both methods (DWIBS<sup>+</sup>PET<sup>+</sup>), disease detectable by DWIBS only (DWIBS<sup>+</sup>PET<sup>-</sup>), or no detectable disease by either method (DWIBS<sup>-</sup>PET<sup>-</sup>). None of the patients was DWIBS-negative but FDG-PET-positive. Four cases with diffuse infiltration patterns in DWIBS and suspected MM involvement in FDG-PET were assigned to the DWIBS<sup>+</sup>PET<sup>+</sup> group to avoid an overestimation of PET false-negativity.

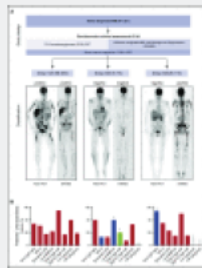
FISH, GEP of CD138-enriched PCs, 70-gene classifier (GEP70)-based risk designation, and molecular subgroup classification were done as previously described.<sup>9-11</sup> Differential gene expression was assessed as published.<sup>12,13</sup> An

expression quantitative trait locus (eQTL) analysis was performed for polymorphisms within 1 MB of the transcription start site of *hexokinase-2* (*HK2*) as described.<sup>14</sup> Copy-number aberrations (CNAs) were called using HumanOmni 2.5 SNP arrays (Illumina) as described.<sup>15</sup>

Wilcoxon or Fisher exact tests were used to compare the median of a continuous variable or the distribution of discrete variables across groups, respectively. Correlation coefficients were determined using Spearman rank correlation. Main analyses were undertaken using R (v3.3.1) software.

## Results and discussion

Of the 227 patients studied, 186 were DWIBS<sup>+</sup>PET<sup>+</sup>. A further group of 15 patients was DWIBS<sup>-</sup>PET<sup>-</sup> ([Figure 1A](#)). Comparing the 2 groups, there was a significantly lower proportion of adverse chromosomal prognostic markers and a trend for a lower tumor burden in DWIBS<sup>-</sup>PET<sup>-</sup>, indicating that in ~7% of patients the tumor burden may be below the detection threshold of both of these imaging modalities ([Figure 1B](#)).



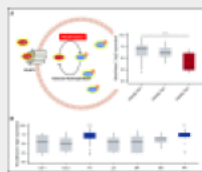
[View larger version](#)

**Figure 1. Study design, imaging results, and patients' characteristics.** (A) Top panel: the study design is shown. Bottom panel: the proportion of patients with specific imaging results and representative paired FDG-PET/DWIBS images. (B) Bars represent the percentage of patients positive for the respective feature. Low BMPCs were defined as  $\leq 20\%$ . Significance of Fisher exact test is illustrated with symbols: + $P < .1$ ; \* $P < .05$ ; \*\* $P < .01$ ; \*\*\*\* $P < .0001$ .

For statistical calculations, the set of DWIBS<sup>+</sup>PET<sup>+</sup> patients was used as reference. BMPC, bone marrow plasma cell infiltration; HY, hyperdiploid; IgG, immunoglobulin G; ISS 3, International Staging System 3; LDH, lactate dehydrogenase; PR, proliferative.

In 11% of patients (26 of 227), we found evidence of disease using DWIBS but no apparent disease involvement using PET (DWIBS<sup>+</sup>PET<sup>-</sup>; [Figure 1A](#)). Of these patients, 5 presented with FLs only, 13 with FLs and diffuse involvement, and 13 with extensive diffuse involvement. There was no difference between the DWIBS<sup>+</sup>PET<sup>+</sup> and this group with regard to parameters associated with tumor load, such as the degree of BMPC infiltration or ISS3. None of the patients with DWIBS<sup>+</sup>PET<sup>-</sup> were assigned to the HY ( $P < .0001$ ) or PR ( $P = .01$ ) molecular subgroup ([Figure 1B](#)), indicating that this imaging pattern was significantly impacted by tumor intrinsic features.

To elucidate the mechanism underlying the “PET false-negativity” phenomenon, we compared GEP data derived from the DWIBS<sup>+</sup>PET<sup>+</sup> and DWIBS<sup>+</sup>PET<sup>-</sup> cases. After correction for multiple testing, we found 21 differentially expressed genes. Interestingly, the gene coding for HK2 was the top differentially expressed gene, with significantly lower expression in false-negative PET cases (fold change, 5.3×;  $P < .001$ ) [Figure 2A](#). There were 5 other differentially expressed genes (upregulated, *DDR1*, *MPZL3*, *NDRG2*, *TMBIM6*; downregulated, *NPM1*) which also play a role in metabolism (supplemental Table 1).



[View larger version](#)

**Figure 2. HK2 expression.** (A) A schema illustrating the functional role of HK2 in the metabolism of FDG (left panel) and a boxplot with the expression level of HK2 in PCs obtained from patients with DWIBS<sup>+</sup>PET<sup>+</sup>, DWIBS<sup>-</sup>PET<sup>-</sup>, and DWIBS<sup>+</sup>PET<sup>-</sup> imaging results (right panel). (B) The plot shows *HK2* expression in PCs stratified by UAMS molecular subgroups.<sup>11</sup>

HK2 catalyzes the first step of glycolysis, the phosphorylation of glucose to hydrophilic glucose-6-phosphate. Like glucose, FDG undergoes phosphorylation by HK2, which prevents back diffusion through the cell membrane.<sup>16</sup> Recently, expression levels of *HK2* were associated with FDG uptake in mouse models of breast cancer, supporting the observations in the current study.<sup>17</sup> We conclude that low expression of *HK2* and the resulting lower levels of metabolically trapped FDG in tumor cells could explain false-negative PET results. *HK2* expression was significantly increased in the HY molecular subgroup, corresponding to the lack of DWIBS<sup>+</sup>PET<sup>-</sup> cases in this subgroup (Figure 2B). Overexpression of glucose-6-phosphatase, which catalyzes the reverse reaction to HK2, mediates false-negative FDG-PET results in hepatocellular carcinoma,<sup>18,19</sup> lending support to our findings of the associations of low *HK2* levels with false-negative FDG-PET.

Next, we aimed to elucidate the mechanism underlying differential *HK2* expression. Although *HK2* expression positively correlated with proliferation (Spearman rank correlation  $\rho = 0.24$ ;  $P < .001$ ), we also found cases with low *HK2* expression but increased proliferation rates, excluding proliferation as a parameter solely explaining low *HK2* expression in PET false-negative patients (supplemental Figure 1). In 7 DWIBS<sup>+</sup>PET<sup>-</sup> cases with available CNAs, we neither detected a CNA involving 2p13, the locus of *HK2*, nor any other shared CNA that could explain this observation. Analyzing an eQTL set<sup>14</sup> including 1449 MM patients, we only found a weak association between the *HK2* common polymorphism rs923273 and *HK2* expression ( $\beta = 0.16 \pm 0.04$ ; supplemental Figure 2), an effect which could not explain a fivefold expression difference. In summary, *HK2*

expression levels were significantly associated with false-negative FDG-PETs, but the mechanism underlying low *HK2* expression remains elusive.

For PET,  $\geq 3$  FLs were previously reported as a poor prognostic marker,<sup>4,5</sup> suggesting that PET negativity could translate into a favorable outcome. However, due to the limited number of DWIBS<sup>+</sup>PET<sup>-</sup> cases, large studies are required to investigate the prognostic impact of this pattern. Interestingly, in a follow-up analysis of DWIBS<sup>+</sup>PET<sup>-</sup> cases, PET-avid disease was seen in 4 of 8 relapsed patients (supplemental Table 2). Future studies will have to investigate the mechanism underlying this apparent change in FDG uptake and also the contribution of the microenvironment.

To overcome the limitations of FDG-PET, alternative tracers have been studied in MM with promising results.<sup>20,21</sup> However, due to the substantial interpatient tumor heterogeneity in MM, alternative tracers could also lead to false-negative results in subsets of patients.

In summary, we demonstrate that at least 10% of patients could be misclassified using FDG-PET as the only functional imaging technology. We describe a strong association between *HK2* expression and this phenomenon in MM, which may also be relevant for the clinical imaging of other hematological cancers.

## Footnotes

The online version of this article contains a data supplement.

The publication costs of this article were defrayed in part by page charge payment. Therefore, and solely to indicate this fact, this article is hereby marked “advertisement” in accordance with 18 USC section 1734.

## **Acknowledgments**

The authors thank the patients and staff of the Myeloma Institute, University of Arkansas for Medical Sciences (UAMS). The authors also thank the Department of Radiology, UAMS.

This work was supported by P01 CA 55819 from the National Cancer Institute, National Institutes of Health. L.R. was supported by the Deutsche Forschungsgemeinschaft (DFG).

## **Authorship**

Contribution: L.R., N.W., E.A., F.E.D., and G.J.M. conceived and designed the study; G.J.M., B.B., F.v.R., M.Z., S.T., C. Schinke, F.E.D., H.G., K.H., and R.H. provided study material or patients; N.W., T.M., and L.R. performed bioinformatic and statistical analyses; E.A., J.E.M., and R.S. reported imaging; L.R., N.W., G.J.M., C.P., and E.A. interpreted data; N.W., L.R., and G.J.M. wrote the paper; and all authors reviewed and approved the paper.

Conflict-of-interest disclosure: B.B. is a co-inventor on patents and patent applications related to use of GEP in cancer medicine that have been licensed to Signal Genetics Inc. The remaining authors declare no competing financial interests.

Correspondence: Leo Rasche, Myeloma Institute, University of Arkansas for Medical Sciences, 4301 W. Markham, #816, Little Rock, AR 72205; e-mail: lrasche@uams.edu.

---

## References

- E TerposMA DimopoulosLA Moulopoulos The role of imaging in the treatment of patients with multiple myeloma in 2016. *Am Soc Clin Oncol Educ Book*. 2016;35:e407-e417.27249748
- Y NonomuraM YasumotoR Yoshimura Relationship between bone marrow cellularity and apparent diffusion coefficient. *J Magn Reson Imaging*. 2001;13(5):757-760.11329198
- C PawlynL FowkesS Otero Whole-body diffusion-weighted MRI: a new gold standard for assessing disease burden in patients with multiple myeloma? *Leukemia*. 2016;30(6):1446-1448.26648535
- E ZamagniF PatriarcaC Nanni Prognostic relevance of 18-F FDG PET/CT in newly diagnosed multiple myeloma patients treated with up-front autologous transplantation. *Blood*. 2011;118(23):5989-5995.21900189
- TB BartelJ HaesslerTL Brown F18-fluorodeoxyglucose positron emission tomography in the context of other imaging techniques and prognostic factors in multiple myeloma. *Blood*. 2009;114(10):2068-2076.19443657
- E ZamagniC NanniF Gay 18F-FDG PET/CT focal, but not osteolytic, lesions predict the progression of smoldering myeloma to active disease. *Leukemia*. 2016;30(2):417-422.26490489

J Hillengass O Landgren Challenges and opportunities of novel imaging techniques in monoclonal plasma cell disorders: imaging “early myeloma”. *Leuk Lymphoma*. 2013;54(7):1355-1363.23289361

S Waheed A Mitchell S Usmani Standard and novel imaging methods for multiple myeloma: correlates with prognostic laboratory variables including gene expression profiling data. *Haematologica*. 2013;98(1):71-78.22733020

J Shaughnessy E Tian J Sawyer High incidence of chromosome 13 deletion in multiple myeloma detected by multiprobe interphase FISH. *Blood*. 2000;96(4):1505-1511.10942398

N Weinhold C J Heuck A Rosenthal Clinical value of molecular subtyping multiple myeloma using gene expression profiling. *Leukemia*. 2016;30(2):423-430.26526987

F Zhan Y Huang S Colla The molecular classification of multiple myeloma. *Blood*. 2006;108(6):2020-2028.16728703

G K Smyth Linear models and empirical bayes methods for assessing differential expression in microarray experiments. *Stat Appl Genet Mol Biol*. 2004;3:Article3.16646809

T Meißner A Seckinger K Hemminki Profound impact of sample processing delay on gene expression of multiple myeloma plasma cells. *BMC Med Genomics*. 2015;8:85.26714877

N Li D C Johnson N Weinhold Multiple myeloma risk variant at 7p15.3 creates an IRF4-binding site and interferes with CDCA7L expression. *Nat Commun*. 2016;7:13656.27882933

N Weinhold C Ashby L Rasche Clonal selection and double-hit events involving tumor suppressor genes underlie relapse in myeloma. *Blood*. 2016;128(13):1735-1744.27516441

G J Kelloff J M Hoffman B Johnson Progress and promise of FDG-PET imaging for cancer patient management and oncologic drug development. *Clin Cancer Res*. 2005;11(8):2785-2808.15837727

J V Alvarez G K Belka T C Pan Oncogene pathway activation in mammary tumors dictates FDG-PET uptake. *Cancer Res*. 2014;74(24):7583-7598.25239452

T Torizuka N Tamaki T Inokuma In vivo assessment of glucose metabolism in hepatocellular carcinoma with FDG-PET. *J Nucl Med*. 1995;36(10):1811-1817.7562048

C Caracó L Aloj L Y Chen J Y Chou W C Eckelman Cellular release of [18F]2-fluoro-2-deoxyglucose as a function of the glucose-6-phosphatase enzyme system. *J Biol Chem*. 2000;275(24):18489-18494.10764804

C Lapa S Knop M Schreder 11C-methionine-PET in multiple myeloma: correlation with clinical parameters and bone marrow involvement. *Theranostics*. 2016;6(2):254-261.26877783

C Lapa M Schreder A Schirbel [(68)Ga]Pentixafor-PET/CT for imaging of chemokine receptor CXCR4 expression in multiple myeloma - comparison to [(18)F]FDG and laboratory values. *Theranostics*. 2017;7(1):205-212.28042328

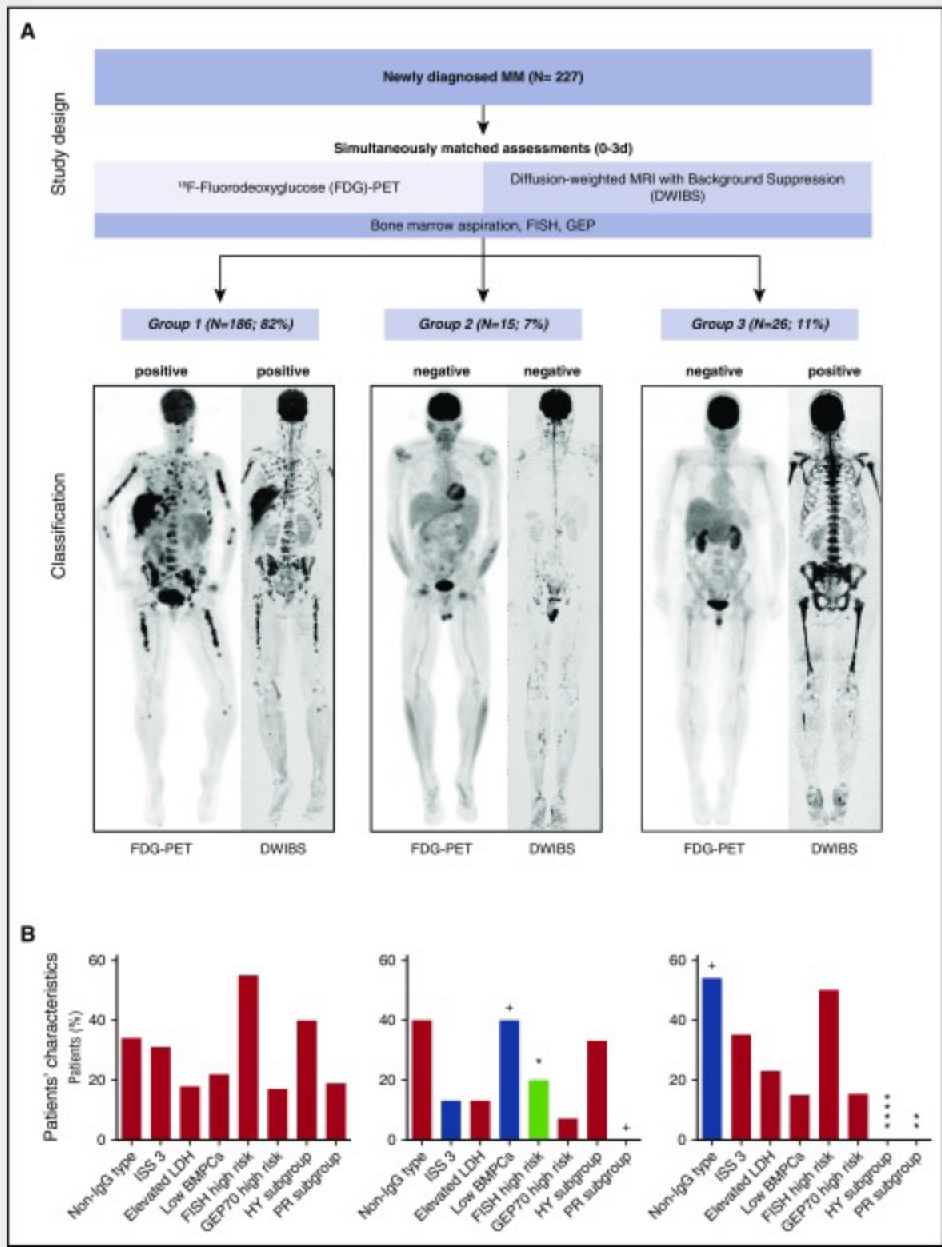


**Figure 1.**

**Study design, imaging results, and patients' characteristics.** (A) Top panel: the study design is shown. Bottom panel: the proportion of patients with specific imaging results and representative paired FDG-PET/DWIBS images. (B) Bars represent the percentage of patients positive for the respective feature. Low BMPCs were defined as  $\leq 20\%$ . Significance of Fisher exact test is illustrated with symbols: + $P < .1$ ; \* $P < .05$ ; \*\* $P < .01$ ; \*\*\*\* $P < .0001$ . For statistical calculations, the set of DWIBS<sup>+</sup>PET<sup>+</sup> patients was used as reference. BMPC, bone marrow plasma cell infiltration; HY,

hyperdiploid; IgG, immunoglobulin G; ISS 3, International Staging System 3; LDH, lactate dehydrogenase; PR, proliferative.

[\[Back\]](#)

[\[Back\]](#)

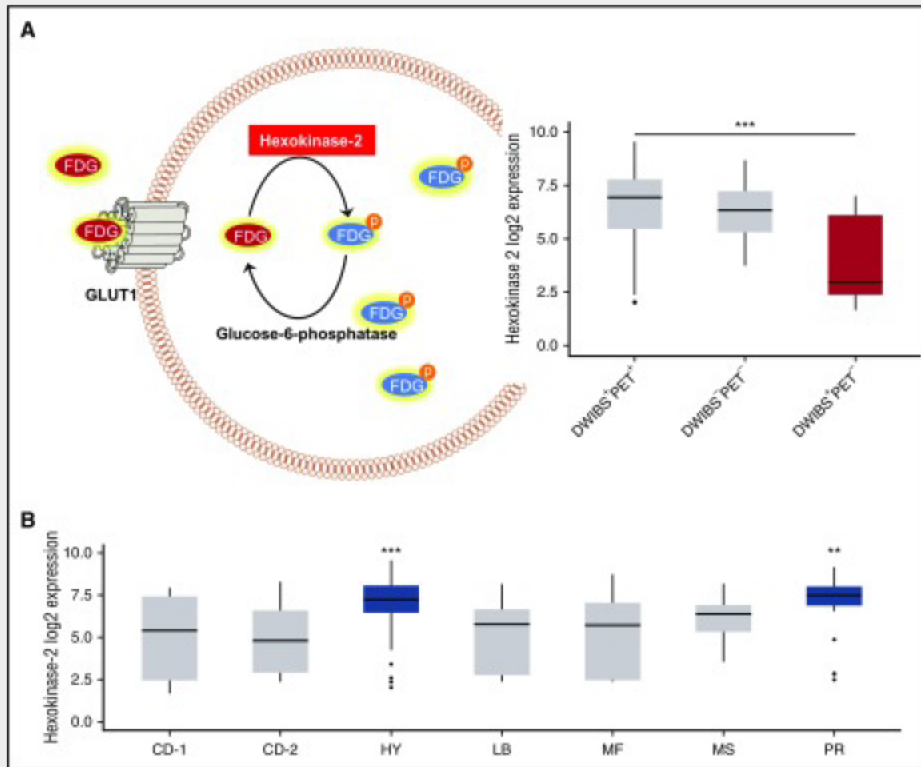


## Figure 2.

**HK2 expression.** (A) A schema illustrating the functional role of HK2 in the metabolism of FDG (left panel) and a boxplot with the expression level of HK2 in PCs obtained from patients with DWIBS<sup>+</sup>PET<sup>+</sup>, DWIBS<sup>-</sup>PET<sup>-</sup>, and DWIBS<sup>+</sup>PET<sup>-</sup> imaging results (right panel). (B) The plot shows *HK2* expression in PCs stratified by UAMS molecular subgroups.<sup>11</sup>

[\[Back\]](#)